© 2021. Published by The Company of Biologists Ltd | Development (2021) 148, dev200178. doi:10.1242/dev.200178

RESEARCH REPORT

DPPA2 and DPPA4 are dispensable for mouse zygotic genome activation and pre-implantation development

Zhiyuan Chen[1,2,3], Zhenfei Xie[1,2,3,*] and Yi Zhang[1,2,3,4,5,‡]

ABSTRACT

How maternal factors in oocytes initiate zygotic genome activation (ZGA) remains elusive in mammals, partly due to the challenge of *de novo* identification of key factors using scarce materials. Two-cell (2C)-like cells have been widely used as an *in vitro* model in order to understand mouse ZGA and totipotency because of their expression of a group of two-cell embryo-specific genes and their simplicity for genetic manipulation. Recent studies indicate that DPPA2 and DPPA4 are required for establishing the 2C-like state in mouse embryonic stem cells in a DUX-dependent manner. These results suggest that DPPA2 and DPPA4 are essential maternal factors that regulate *Dux* and ZGA in embryos. By analyzing maternal knockout and maternal-zygotic knockout embryos, we unexpectedly found that DPPA2 and DPPA4 are dispensable for *Dux* activation, ZGA and pre-implantation development. Our study suggests that 2C-like cells do not fully recapitulate two-cell embryos in terms of regulation of two-cell embryo-specific genes, and, therefore, caution should be taken when studying ZGA and totipotency using 2C-like cells as the model system.

KEY WORDS: Zygotic genome activation, *Dux*, *Dppa2/4*, 2C-like, Two-cell embryo, Pre-implantation development

INTRODUCTION

Following fertilization, embryonic development relies initially on maternal factors deposited during oogenesis and subsequently on the newly generated embryonic product after its genome is activated. The awakening of the embryonic genome is known as zygotic or embryonic genome activation (ZGA/EGA), which is essential for an embryo to acquire totipotency and to undergo normal development. In mice, ZGA consists of two successive waves of transcription – a minor and a major wave occurring at the late one-cell and late two-cell stages, respectively (Schultz et al., 2018). Transcription at the late one-cell stage is largely promiscuous and splicing and 3′ processing of the transcripts are largely incomplete (Abe et al., 2015), whereas the major ZGA at the late two-cell stage involves the expression of thousands of translatable mRNAs (Hamatani et al., 2004; Wang et al., 2004; Zeng et al., 2004). Notably, both minor and major ZGA are essential for mouse pre-implantation development (Abe et al., 2018; Schultz et al., 2018; Liu et al., 2020).

Two-cell (2C)-like cells are a rare cell subpopulation of embryonic stem cells (ESCs) that is characterized by the expression of many transcripts that are specific to two-cell embryos, such as *Zscan4* and *Zfp352*, and has the expanded potential to contribute to both embryonic and extra-embryonic lineages (Macfarlan et al., 2012). 2C-like cells have been widely used as an *in vitro* system in which to study totipotency and ZGA (Fu et al., 2020; Genet and Torres-Padilla, 2020). Studies in the past several years have identified DUX (human homolog DUX4), a double homeodomain protein, as a master regulator of the 2C-like state in ESCs (De Iaco et al., 2017; Hendrickson et al., 2017; Whiddon et al., 2017). Most of the mechanisms that promote the 2C-like state in ESCs identified so far directly or indirectly regulate *Dux* activation. Intriguingly, loss of *Dux* in embryos only mildly affects ZGA and *Dux* null embryos are viable with reduced litter sizes (Chen and Zhang, 2019; Guo et al., 2019; De Iaco et al., 2020; Bosnakovski et al., 2021). Thus, although DUX is important for synchronizing and enhancing the expression of some 2C embryo-specific genes, it is not essential for ZGA and embryogenesis.

Given that *Dux* is not expressed in oocytes and it gets activated only at the late one-cell stage, upstream factors must have already been expressed in oocytes in order to trigger *Dux* expression during the minor ZGA wave. Recent studies have identified developmental pluripotency associated 2 and 4 (DPPA2 and DPPA4) as essential factors for establishing the 2C-like state in ESCs by activating *Dux* (De Iaco et al., 2019; Eckersley-Maslin et al., 2019; Yan et al., 2019). In addition, DPPA2 and DPPA4 directly regulate young LINE-1 elements in ESCs in a DUX-independent manner (De Iaco et al., 2019). The young LINE-1 elements levels also increase during the major ZGA wave. Taken together, these findings suggest that DPPA2 and DPPA4, which are expressed in oocytes, may regulate ZGA as maternal factors through both DUX-dependent and -independent pathways. In support of this, overexpression of the dominant-negative forms of *Dppa2* has been shown to impair mouse pre-implantation development (Hu et al., 2010; Yan et al., 2019). However, because overexpression of dominant-negative forms might cause unknown side effects, these two studies did not provide definite evidence for *Dppa2/4* function in ZGA. In addition, the previous *Dppa2* and *Dppa4* zygotic knockout (KO) studies (Madan et al., 2009; Nakamura et al., 2011) did not address the potential maternal contributions of these two proteins in ZGA and pre-implantation development. Thus, whether oocyte-derived DPPA2 and DPPA4 activate *Dux* expression and regulate ZGA in mouse embryos remains to be formally confirmed.

In this study, we generated maternal KO and maternal-zygotic KO mouse embryos for both *Dppa2* and *Dppa4*, and determined their

[1]Howard Hughes Medical Institute, Boston Children's Hospital, Boston, Massachusetts 02115, USA. [2]Program in Cellular and Molecular Medicine, Boston Children's Hospital, Boston, Massachusetts 02115, USA. [3]Division of Hematology/Oncology, Department of Pediatrics, Boston Children's Hospital, Boston, Massachusetts 02115, USA. [4]Department of Genetics, Harvard Medical School, Boston, Massachusetts 02115, USA. [5]Harvard Stem Cell Institute, WAB-149G, 200 Longwood Avenue, Boston, Massachusetts 02115, USA.
*Present address: The Ragon Institute of Massachusetts General Hospital, Massachusetts Institute of Technology and Harvard University, Cambridge, MA 02139, USA.

‡Author for correspondence (yzhang@genetics.med.harvard.edu)

Z.C., 0000-0002-6756-1895; Y.Z., 0000-0002-2789-0811

Handling Editor: Patrick Tam
Received 8 September 2021; Accepted 25 November 2021

Development (2021) 148, dev200178. doi:10.1242/dev.200178

functions in *Dux* activation, ZGA and pre-implantation development. Our results demonstrate that both DPPA2 and DPPA4 are dispensable for ZGA and pre-implantation development.

RESULTS AND DISCUSSION

Expression dynamics of *Dppa2* and *Dppa4* in mouse early development

To test the possibility that DPPA2 and DPPA4 are involved in activating *Dux* expression and ZGA, we first determined the expression dynamics and cellular localization of these proteins in early embryos by RNA sequencing (RNA-seq) and immunostaining analyses. We found that low levels of *Dppa2* and *Dppa4* RNAs were detectable in both oocytes and zygotes, and their expression levels were dramatically increased during major ZGA and reached a peak at the eight-cell stage (Fig. 1A). However, both *Dppa2* and *Dppa4* RNA became undetectable soon after embryo implantation (Fig. 1A); this transcriptional silencing is presumably achieved by gain of DNA methylation at the promoters (Eckersley-Maslin et al., 2019).

In contrast to the RNA levels, DPPA2 and DPPA4 immunosignals were not detectable in either oocytes or zygotes (Fig. 1B,C). Signals were first detectable at the late two-cell stage and became stronger at subsequent stages (Fig. 1B,C). At the blastocyst stage, DPPA2 and DPPA4 were mostly located in the inner cell mass (i.e. NANOG positive) rather than trophectoderm (i.e. CDX2-positive cells) (Fig. 1D). This observation is consistent with previous RNA *in situ* hybridization experiments showing that *Dppa2* and *Dppa4* are restricted to the inner cell mass at this stage (Maldonado-Saldivia et al., 2007).

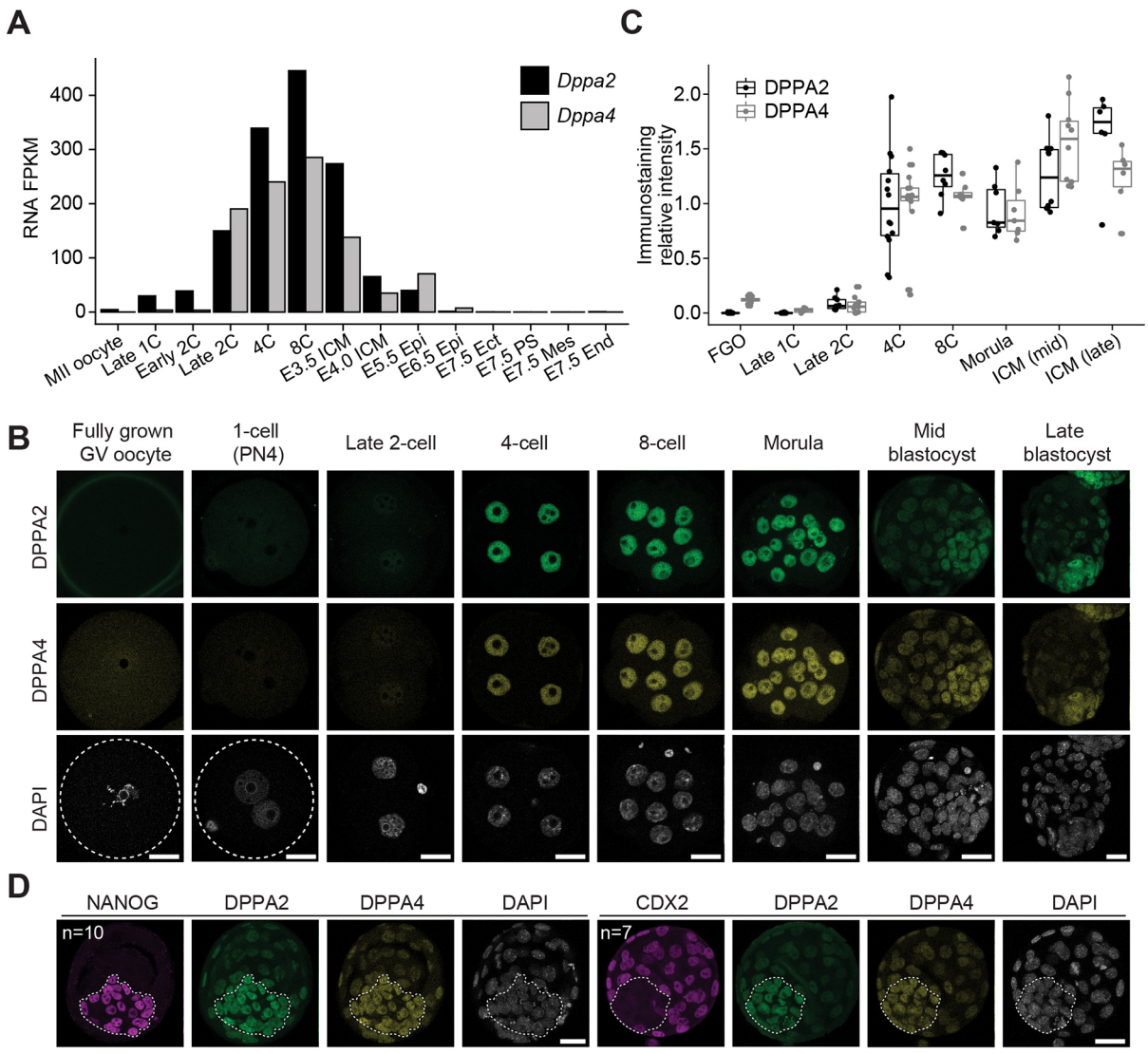

Fig. 1. Expression and cellular localization of DPPA2 and DPPA4 in mouse oocytes and early embryos. (A) RNA levels of *Dppa2* and *Dppa4* in oocyte and early embryos. The RNA-seq data were taken from previously published studies (Wu et al., 2016; Zhang et al., 2018). Ect, ectoderm; End, endoderm; Epi, epiblast; ICM, inner cell mass; Mes, mesoderm; PS, primitive streak. (B) Images of oocytes and pre-implantation embryos immunostained with antibodies against DPPA2 and DPPA4. GV, germinal vesicle; PN, pronucleus. (C) Quantification of the signal intensities of DPPA2 and DPPA4. The average signal intensities of four-cell embryos were set as 1.0. The total number of oocytes/embryos analyzed were 13 for oocytes, eight for one-cell embryos, nine for two-cell embryos, 14 for 4-cell embryos, eight for eight-cell embryos, seven for morulae, ten for mid blastocysts, and six for late blastocysts. The middle lines represent medians. The box hinges indicate the 25th and 75th percentiles, and the whiskers indicate the hinge±1.5×interquartile range. FGO, fully grown GV oocytes. (D) Images of blastocysts immunostained with antibodies against DPPA2, DPPA4, NANOG and CDX2. Number of embryos analyzed are as labeled. Dotted lines delineate ICM. Scale bars: 20 µm.

Development (2021) 148, dev200178. doi:10.1242/dev.200178

Generation of *Dppa2* and *Dppa4* maternal and maternal-zygotic KO embryos

The immunostaining results are incompatible with a potential role of DPPA2 and DPPA4 in *Dux* activation and ZGA in embryos. However, it is also possible that the very low levels of maternal DPPA2 and DPPA4 proteins in oocytes (barely detected by immunostaining) may still play a role in activating *Dux* and ZGA. To test this possibility, we generated *Gdf9-Cre*-mediated oocyte-specific conditional KO (CKO) models for *Dppa2* (exon 3-4 floxed) (Fig. 2A) and *Dppa4* (exon 2-7 floxed) (Fig. 2B). The *Gdf9-Cre* is expressed in early growing oocytes around postnatal day 3 (Lan et al., 2004). As the *Dppa4* flox (*fl*) allele has been previously established and described (Nakamura et al., 2011), we only characterized in detail the *Dppa2 fl* allele that was generated in this study using the two-cell homologous recombination (2C-HR)-CRISPR method (Gu et al., 2018) (Fig. S1A,B). Sanger sequencing analyses confirmed that exons 3 and 4 of *Dppa2* were successfully depleted in the CKO oocytes (Fig. S1C), resulting in a frameshift disrupting both the SAP and C-terminal domains. Because *Dppa2* and *Dppa4* are closely linked on the same chromosome, it is not feasible to generate *Dppa2* and *Dppa4* double CKO mice by natural mating.

We next sought to confirm successful knock out of DPPA2 and DPPA4 at the protein level. Because of the weak DPPA2 and DPPA4 immunostaining signals before the four-cell stage (Fig. 1B), it was challenging to determine their reduction in CKO oocytes and maternal KO one-cell/two-cell embryos. To circumvent this issue, immunostaining analyses were performed at the four-cell stage for maternal KO (*m−z+*) and maternal-zygotic KO (*m−z−*) embryos generated by crossing CKO female mice with heterozygous male mice (Fig. 2C). DPPA2 and DPPA4 signal intensities in maternal KO four-cell embryos were largely comparable to that of wild-type (WT) embryos (Fig. 2C, Fig. 1B). This suggests that *Dppa2* and *Dppa4* were zygotically expressed from the WT paternal alleles, which compensated for the maternal loss. In contrast, DPPA2 and DPPA4 signals were not detectable in *m−z−Dppa2* and *m−z−Dppa4* four-cell embryos, respectively (Fig. 2C,D), confirming the successful knock out of these proteins. It is worth noting that loss of one protein caused reduced signal of the other in maternal-zygotic KO four-cell embryos, albeit to different extents (Fig. 2C,D). This is perhaps due to the fact that DPPA2 and DPPA4 function as a heterodimer (Nakamura et al., 2011; Hernandez et al., 2018) and loss of one may therefore affect the stability of the other, as has been observed in ESCs (Gretarsson and Hackett, 2020).

DPPA2 and DPPA4 are not required for pre-implantation development

Having confirmed the successful knock out of DPPA2 and DPPA4 in embryos, we next examined the impact of DPPA2 and DPPA4

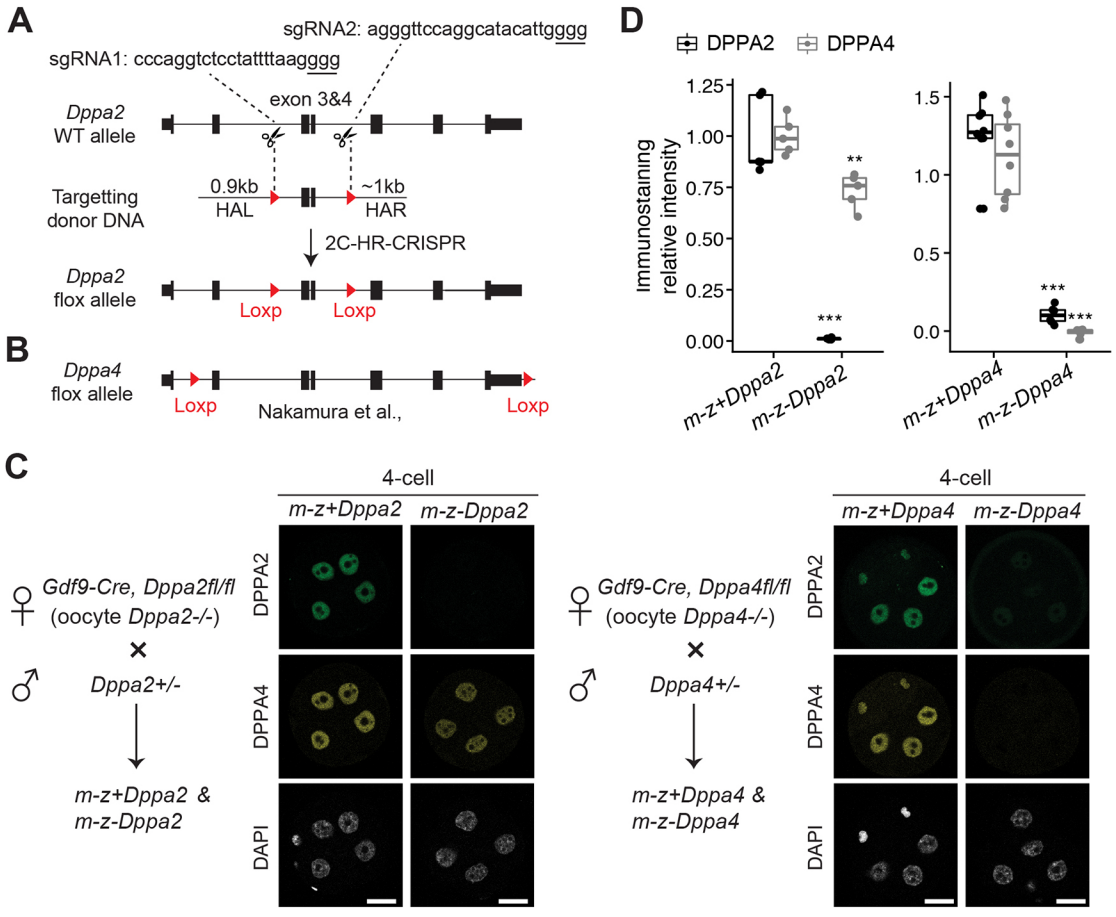

Fig. 2. Generation of maternal KO (*m−z+*) and maternal-zygotic KO (*m−z−*) embryos for *Dppa2* and *Dppa4*. (A) Gene targeting strategy for *Dppa2* flox allele. HAL, left homologous arm; HAR, right homologous arm; HR, homologous recombination. (B) Schematic of the *Dppa4* flox allele (Nakamura et al., 2011). (C) Schematics for generating *m−z+* and *m−z−* embryos and images of four-cell embryos immunostained with antibodies against DPPA2 and DPPA4. (D) Quantifications of signal intensities of DPPA2 and DPPA4. The average signal intensities of *m−z+* embryos were set as 1.0. The number of embryos analyzed were five for *m−z+Dppa2*, five for *m−z−Dppa2*, eight for *m−z+Dppa4* and six for *m−z−Dppa4*. The middle lines represent medians. The box hinges indicate the 25th and 75th percentiles, and the whiskers indicate the hinge±1.5×interquartile range. ***P<0.001, **P<0.01 (two-tailed Student's t-test).

Development (2021) 148, dev200178. doi:10.1242/dev.200178

knock out on pre-implantation development. To this end, spermatozoa from WT male mice were used to fertilize oocytes from control and CKO female mice *in vitro*, generating WT (*m+z+*) and maternal KO (*m−z+*) embryos. To exclude the possibility of the WT paternal copy compensating for the maternal losses, CKO oocytes were also fertilized with heterozygous spermatozoa, which should generate maternal-zygotic KO (*m−z−*) in half of the embryos. Unexpectedly, none of the embryo groups showed apparent pre-implantation defects and *m−z−* blastocysts were identified by immunostaining at the expected Mendelian ratio (Fig. 3A,B). It should be noted that loss of both DPPA2 and DPPA4 in *m−z−Dppa4* blastocysts makes these embryos equivalent to *Dppa2/4* double KO (Fig. 3B). Importantly, analyses of *in vivo* blastocysts collected after natural mating also led to the same observations (Fig. 3C,D, Fig. S2A). In summary, these results indicate that DPPA2 and DPPA4 are not required for mouse pre-implantation development.

Having confirmed the dispensable role of DPPA2/4 in pre-implantation development, we next examined whether they are required for post-implantation development. Mating analyses revealed that, although maternal DPPA2 or DPPA4 is not required for development, few *m−z−Dppa2* and *m−z−Dppa4* developed to weaning stage (Fig. S2B). Lethality of *m−z−* mutants should occur around or after birth because a close-to-Mendelian ratio was

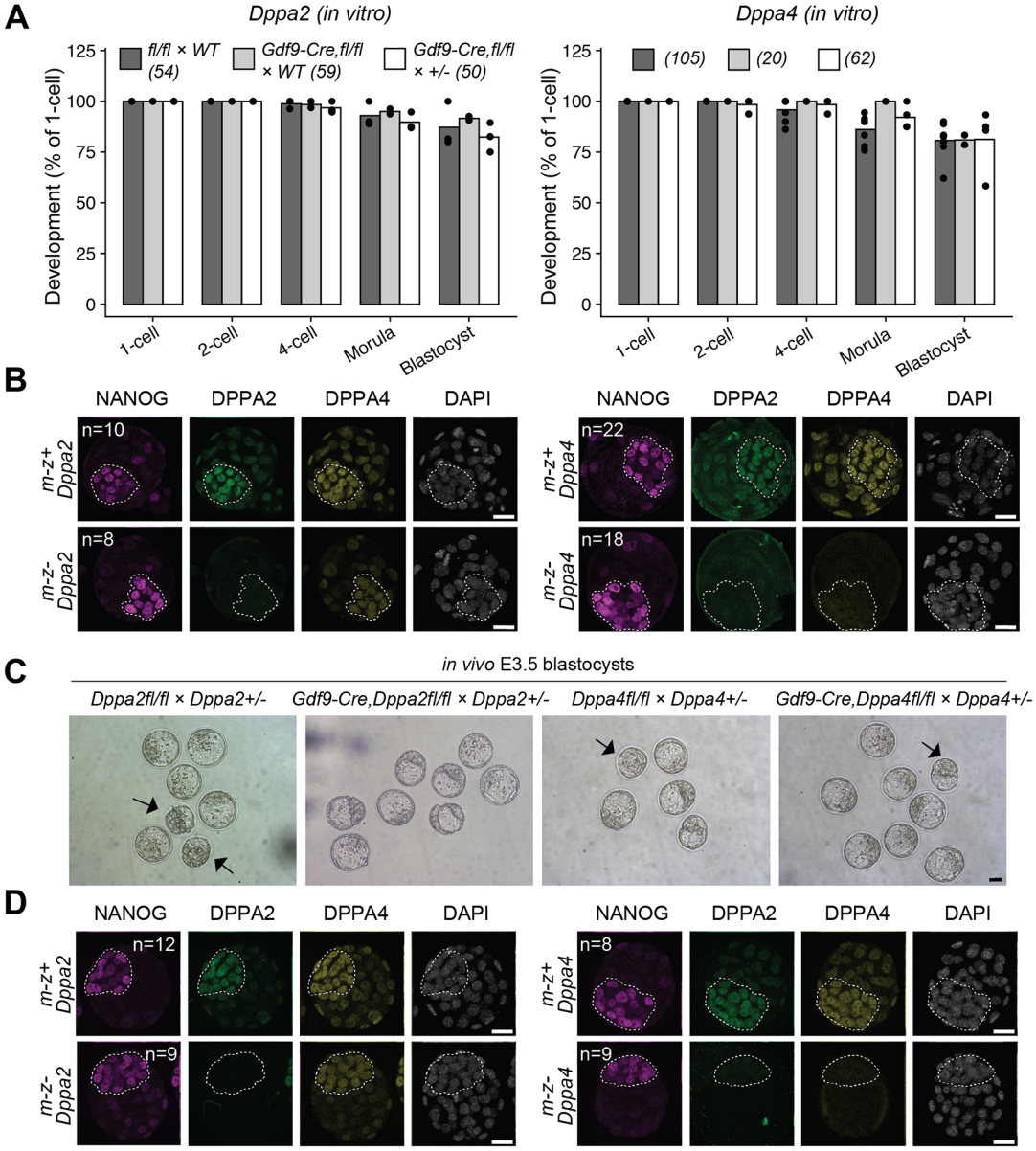

Fig. 3. Embryos without DPPA2 and DPPA4 undergo normal pre-implantation development. (A) Bar graphs showing the percentage of *in vitro*-fertilized one-cell embryos reaching the indicated developmental stages when cultured *in vitro*. Circles represent individual experiments. Total number of embryos analyzed for each group are shown in parentheses. A subset of blastocysts were genotyped by immunostaining (shown in B). (B) Images of *in vitro* blastocysts immunostained with antibodies against NANOG, DPPA2 and DPPA4. The numbers of embryos with the indicated genotypes are as shown. (C) Representative images of E3.5 blastocysts flushed from reproductive tracts after natural mating. Each image was obtained from one litter. Arrows point to the not fully expanded blastocysts, which were found in both control and CKO groups. See Fig. S2A for a summary of all the *in vivo* blastocysts collected. (D) Images of *in vivo* blastocysts immunostained with antibodies against NANOG, DPPA2 and DPPA4. The numbers of embryos with indicated genotypes are as shown. Dotted lines in B,D delineate ICM. Scale bars: 20 µm.

Development (2021) 148, dev200178. doi:10.1242/dev.200178

observed at embryonic day (E) 18.5 (Fig. S2B). However, the *m−z−* mutants already showed some phenotypes, including smaller sizes and/or pale skins by E18.5 (Fig. S2C). These data suggest that loss of maternal-zygotic DPPA2 or DPPA4 causes perinatal lethality, which is very similar to the effect of zygotic knockouts of DPPA2 and/or DPPA4 previously reported (Madan et al., 2009; Nakamura et al., 2011). Thus, DPPA2 and/or DPPA4 are essential for post-implantation, but not pre-implantation, development.

DPPA2 and DPPA4 are dispensable for *Dux* expression and ZGA

Given that mouse pre-implantation development is largely normal without DPPA2 or DPPA4, minimal ZGA defects are expected in these mutants. To confirm this prediction, we performed RNA-seq experiments. To determine whether DPPA2 and DPPA4 initiate *Dux* transcription during minor ZGA and subsequently affect major ZGA, late one-cell and late two-cell embryos of control and maternal KO were collected for RNA-seq analyses (Fig. S3A). Maternal-zygotic KO single two-cell embryos were also analyzed to exclude the possibility of the WT paternal allele in *m−z+* embryos compensating for the maternal loss (Fig. S3B). All RNA-seq biological replicates were highly reproducible (Fig. S3A,B), and the RNA-seq genome browser views confirmed the success of Cre-mediated depletion of *Dppa2* and *Dppa4* in the *m−z+* late one-cell (Fig. S4A) and *m−z−* late two-cell embryos (Fig. 4A).

We next performed comparative analyses in *m+z+*, *m−z+*, and *m−z−* embryos to identify differentially expressed genes [fragments per kilobase of transcript per million mapped reads (FPKM) >1, fold change (FC) >2, and adjusted *P*-value<0.05]. As expected, minimal changes in gene/repeat expression were observed in both *m−z+* and *m−z−* mutant embryos (Fig. S4B,C, Fig. 4B, Tables S1 and S2). Note that both *Dux* and its target genes/repeats, such as *Zscan4*, *Zfp352*, *MERVL-int* and *MT2_Mm* were normally activated during minor and major ZGA. In addition, the young LINE-1 elements, including *L1Md_A* and *L1Md_T*, which are regulated by DPPA2 and DPPA4 independently of DUX in ESCs (De Iaco et al., 2019), were also normally expressed in late two-cell embryos (Fig. S4C, Fig. 4B). Consistent with minimal transcriptome alterations, the major ZGA genes (*n*=2470, two-cell/one-cell: FC>5, FPKM>3, adjusted *P*-value<0.05), including those previously reported to be regulated by DPPA2 and DPPA4 in ESCs, also showed normal activation (Fig. 4C,D, Fig. S4D). Thus, our data support the suggestion that DPPA2 and DPPA4 are dispensable for *Dux* expression and ZGA in mouse early embryos.

Collectively, our data provide definite evidence that maternal DPPA2 and DPPA4 are not required to trigger the activation of *Dux* and other two-cell embryo-specific genes during mouse ZGA. Although generation of double KOs were not feasible by natural mating owing to their close genetic linkage, DPPA2 and DPPA4 should not compensate for each other for the following reasons. First, DPPA2 and DPPA4 function as a heterodimer (Nakamura et al., 2011; Hernandez et al., 2018). Loss of either protein causes comparable phenotypes to the double KOs during both ESC differentiation (i.e. failure of developmental gene activation) (Eckersley-Maslin et al., 2020; Gretarsson and Hackett, 2020) and embryogenesis (i.e. lung developmental defects and perinatal lethality) (Madan et al., 2009; Nakamura et al., 2011). Second, our immunostaining analyses indicated that DPPA2 became almost undetectable when DPPA4 was depleted in early embryos (Fig. 2C and Fig. 3B,D), suggesting that similar results are expected in the maternal-zygotic double KO. Therefore, compensation for each other should not explain the lack of apparent pre-implantation phenotype for the *Dppa2* and *Dppa4* mutants analyzed in this study.

Together with the evidence that DUX does not initiate ZGA in embryos (Chen and Zhang, 2019; Guo et al., 2019; De Iaco et al., 2020; Bosnakovski et al., 2021), this study further highlights the key differences between 2C-like cells and two-cell embryos. In ESCs, both DUX and the DPPA2/4 heterodimer are essential for establishing the 2C-like state (De Iaco et al., 2017; Hendrickson et al., 2017; De Iaco et al., 2019; Eckersley-Maslin et al., 2019; Yan et al., 2019). However, this is not the case in mouse embryos. Therefore, conclusions drawn from 2C-lilke cells should be carefully considered before being applied to the embryo scenario. Recently, TP53 (TRP53 in mouse) has been identified as a maternal factor that regulates DUX and 2C genes in both ESCs and embryos (Grow et al., 2021; Sun et al., 2021). Nonetheless, *Dux* also gets activated in *Tp53* maternal-zygotic KO embryos, although to a lesser extent than in WT (Grow et al., 2021). Thus, multiple pioneer factors may exist to trigger *Dux* and/or other minor ZGA genes (Kobayashi and Tachibana, 2021).

Despite DPPA2 and DPPA4 being dispensable for ZGA, they may be required for maintaining a permissive chromatin state during gastrulation by counteracting DNA methylation, as suggested by the studies in ESCs (Eckersley-Maslin, 2020; Eckersley-Maslin et al., 2020; Gretarsson and Hackett, 2020). Indeed, our data revealed a perinatal lethality phenotype in *Dppa2* and *Dppa4* maternal-zygotic KOs, which is largely similar to the previously reported *Dppa2* and/or *Dppa4* zygotic KO mutants. It is likely that loss of DPPA2 and DPPA4 may cause epigenomic defects around gastrulation, which ultimately contribute to the perinatal lethality phenotype (Madan et al., 2009; Nakamura et al., 2011). This hypothesis warrants further examination.

MATERIALS AND METHODS

Collection of mouse oocytes and pre-implantation embryos

All animal studies were performed in accordance with guidelines of the Institutional Animal Care and Use Committee at Harvard Medical School. The procedures of GV and MII oocytes collection and *in vitro* fertilization were described previously (Chen and Zhang, 2019; Zhang et al., 2020). For all experiments, 6- to 9-week-old mice were used. The *in vitro*-fertilized embryos were cultured in KSOM (Millipore) at 37°C under 5% CO_2 with air. The *in vivo* blastocysts were collected by flushing reproductive tracts at E3.5. The day of vaginal plug was counted as E0.5.

Generation of *Dppa2* and *Dppa4* mutant oocytes and embryos

The *Gdf9-Cre* transgenic line and the *Dppa4 fl* line were described previously (Lan et al., 2004; Nakamura et al., 2011). The *Dppa2 fl* allele was generated by the 2C-HR-CRISPR method (Gu et al., 2018). Specifically, *Cas9* mRNA (100 ng/µl), two sgRNAs (80 ng/µl each), and donor DNA PCR fragment (no biotin) (25 ng/µl) were co-injected into the cytoplasm of each two-cell blastomere using a Piezo impact-driven micromanipulator (Prime Tech). A PCR fragment with ∼0.9-1 kb homologous arms was used because high knock-in efficiency was reported for this donor DNA preparation method (Yao et al., 2018). After injection, the embryos were cultured for a few hours before being transferred into oviducts of surrogate ICR strain mothers. The synthesis of *Cas9* mRNA and sgRNA was described previously (Wang et al., 2013). The donor DNA targeting vector was cloned using the Gibson Assembly method and the primers used for cloning are listed in Table S3. The *Dppa2 fl* F_0 mice (BDF1×BDF1) (The Jackson Laboratory, #100006) were crossed with B6 (The Jackson Laboratory, #000664) to confirm germline transmission.

The breeding schemes were the same for *Dppa2* and *Dppa4* lines. Specifically, the *+/fl* lines were crossed with *Gdf9-Cre* to obtain *Gdf9-Cre, +/fl* males. The *Gdf9-Cre, +/fl* males were then crossed with *+/fl* females to obtain *Gdf9-Cre, fl/fl* males and *fl/fl* females. They were then crossed to

Development (2021) 148, dev200178. doi:10.1242/dev.200178

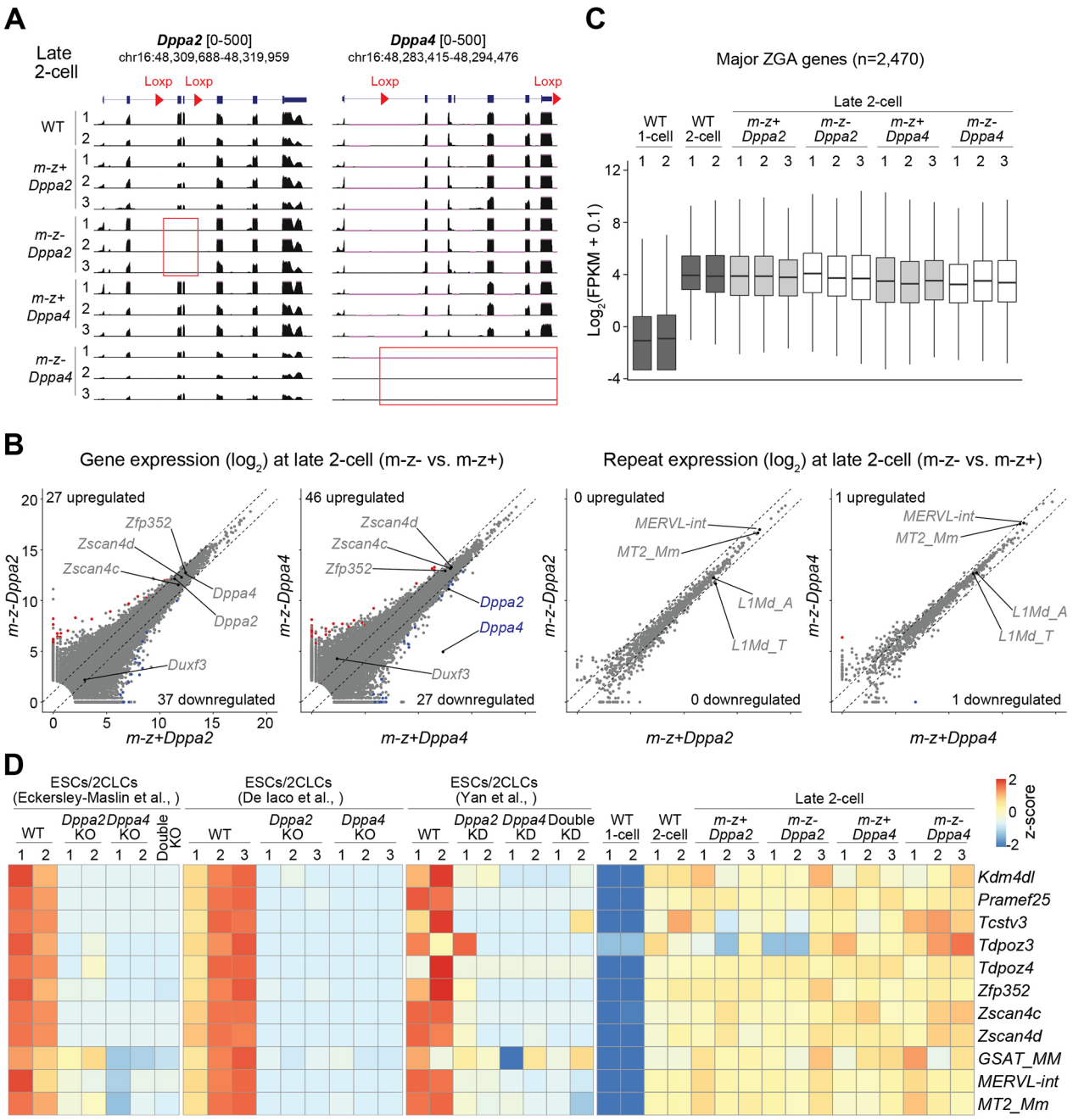

Fig. 4. *Dppa2* and *Dppa4* maternal-zygotic KO embryos undergo normal ZGA. (A) Genome browser views of the indicated RNA-seq samples at *Dppa2* and *Dppa4* loci. Cre-mediated deletion of exons are highlighted by red boxes. (B) Scatter plots comparing gene/repeat expression levels of two-cell embryos (*m−z−* versus *m−z+*). The *x*- and *y*-axes are normalized read counts by DESeq2 (log2) (Love et al., 2014). Differential gene expression criteria were: FC>2, adjusted *P*-value<0.05 and FPKM>1. (C) Boxplot illustrating the expression levels of major ZGA genes of the indicated samples. The major ZGA genes were defined using the following cutoffs: two-cell/one-cell FC>5, two-cell FPKM>3, adjusted *P*-value<0.05. The middle lines represent medians. The box hinges indicate the 25th and 75th percentiles, and the whiskers indicate the hinge±1.5×interquartile range. (D) Heatmap illustrating the expression levels of example genes/repeats in ESCs/2C-like cells (2CLCs) and two-cell embryos. The RNA-seq data of ESCs/2CLCs were from previously published studies (De Iaco et al., 2019; Eckersley-Maslin et al., 2019; Yan et al., 2019).

generate *fl/fl* (control) and *Gdf-Cre, fl/fl* females (CKO) for experiments. Male mice that were heterozygous for Cre-mediated depletions were obtained by crossing *Gdf9-Cre, +/fl* females with WT B6 males. For all mouse lines, tail tips were used for genotyping using the primers listed in Table S3.

Whole-mount immunostaining

Immunostaining, image acquisition, and analyses were performed as previously described (Inoue et al., 2018). Primary and secondary antibodies are listed in Table S3.

RNA-seq libraries preparation and data processing

Reverse-stranded total RNA-seq libraries (Fig. S4, Fig. S3A) were prepared using the SMARTer-Seq Stranded kit (Takara Bio) following the manufacturer's instructions. For single-embryo RNA-seq (Fig. 4, Fig. S3B), cDNA was synthesized using the SMARTer Ultra low Input RNA cDNA preparation kit (Takara Bio). The cDNA was then used for genotyping by quantitative PCR (primers in Table S3) and three embryos for each genotype (i.e. *m−z+* or *m−z−*) were selected for library construction using the Nextera XT DNA Library Preparation Kit (Illumina).

The single-embryo RNA-seq libraries were non-stranded and only PolyA+ RNA was captured. For all RNA-seq libraries, paired-end 75-bp sequencing was performed on a NextSeq 550 sequencer (Illumina). A summary of the generated data sets is available in Table S2.

The total RNA-seq (Fig. S4) and polyA RNA-seq (Fig. 4) data were processed following the pipelines as previously described (Chen and Zhang, 2019; Chen et al., 2021). Briefly, RNA-seq reads were trimmed to remove low quality reads and adaptors using Trimgalore (v0.4.5) before being aligned to mm10 assembly using HISAT2 (v.2.1.0) (Kim et al., 2015). StringTie (v1.3.3b) was used to quantify gene FPKM values (Pertea et al., 2016). For differential expression analyses, DESeq2 (v1.24.0) (Love et al., 2014) was used to compute adjusted *P*-values on read counts generated by TEtranscripts (v. 2.1.4) (Jin et al., 2015). TEtranscripts summarizes only uniquely aligned reads for genes and both uniquely and ambiguously (i.e. due to multiple insertions of repeats) mapped reads for transposable elements. RNA-seq pipeline and data processing R-codes are available at Github (https://github.com/YiZhang-lab/Nonessential_role_of_Dppa2_4_in_ZGA).

The RNA-seq data generated in this study have been deposited in the Gene Expression Omnibus under accession number GSE181723. The RNA-seq data of mouse oocytes and early embryos (Fig. 1A) were from GSE66582 (Wu et al., 2016) and GSE76505 (Zhang et al., 2018). The RNA-seq data of ESCs presented in Fig. 4 and Fig. S4 were from GSE120952 (Eckersley-Maslin et al., 2019), GSE126621 (De Iaco et al., 2019) and GSE127811 (Yan et al., 2019).

Statistical analyses and data visualization

Statistical analyses were performed in R (www.r-project.org/). All sequencing tracks were visualized using the UCSC genome browser (Kent et al., 2002).

Acknowledgements

We thank Dr Yota Hagihara for his help in some immunostaining experiments; Drs Chunxia Zhang, Wenhao Zhang, Yota Hagihara and Cheng-Jie Zhou for critical reading of the manuscript.

Competing interests

The authors declare no competing or financial interests.

Author contributions

Conceptualization: Z.C., Z.X., Y.Z.; Methodology: Z.C., Z.X.; Validation: Z.C.; Formal analysis: Z.C.; Investigation: Z.C.; Resources: Y.Z.; Data curation: Z.C.; Writing - original draft: Z.C.; Writing - review & editing: Z.X., Y.Z.; Visualization: Z.C.; Supervision: Y.Z.; Project administration: Y.Z.; Funding acquisition: Y.Z.

Funding

This project was supported by the National Institutes of Health (R01HD092465) and the Howard Hughes Medical Institute. Y.Z. is an Investigator of the Howard Hughes Medical Institute. Z.C. is currently supported by the Eunice Kennedy Shriver National Institute of Child Health and Human Development (K99HD104902). Deposited in PMC for release after 12 months.

Data availability

The RNA-seq data generated in this study have been deposited in the Gene Expression Omnibus under accession number GSE181723. RNA-seq pipeline and data processing R-codes are available at Github (https://github.com/YiZhang-lab/Nonessential_role_of_Dppa2_4_in_ZGA).

Peer review history

The peer review history is available online at https://journals.biologists.com/dev/article-lookup/doi/10.1242/dev.200178.

References

Abe, K., Yamamoto, R., Franke, V., Cao, M., Suzuki, Y., Suzuki, M. G., Vlahovicek, K., Svoboda, P., Schultz, R. M. and Aoki, F. (2015). The first murine zygotic transcription is promiscuous and uncoupled from splicing and 3′ processing. *EMBO J.* **34**, 1523-1537. doi:10.15252/embj.201490648

Abe, K.-I., Funaya, S., Tsukioka, D., Kawamura, M., Suzuki, Y., Suzuki, M. G., Schultz, R. M. and Aoki, F. (2018). Minor zygotic gene activation is essential for mouse preimplantation development. *Proc. Natl. Acad. Sci. U.S.A.* **115**, E6780-E6788. doi:10.1073/pnas.1804309115

Bosnakovski, D., Gearhart, M. D., Ho Choi, S. and Kyba, M. (2021). Dux facilitates post-implantation development, but is not essential for zygotic genome activation. *Biol. Reprod.* **104**, 83-93. doi:10.1093/biolre/ioaa179

Chen, Z. and Zhang, Y. (2019). Loss of DUX causes minor defects in zygotic genome activation and is compatible with mouse development. *Nat. Genet.* **51**, 947-951. doi:10.1038/s41588-019-0418-7

Chen, Z., Djekidel, M. N. and Zhang, Y. (2021). Distinct dynamics and functions of H2AK119ub1 and H3K27me3 in mouse preimplantation embryos. *Nat. Genet.* **53**, 551-563. doi:10.1038/s41588-021-00821-2

De Iaco, A., Planet, E., Coluccio, A., Verp, S., Duc, J. and Trono, D. (2017). DUX-family transcription factors regulate zygotic genome activation in placental mammals. *Nat. Genet.* **49**, 941-945. doi:10.1038/ng.3858

De Iaco, A., Coudray, A., Duc, J. and Trono, D. (2019). DPPA2 and DPPA4 are necessary to establish a 2C-like state in mouse embryonic stem cells. *EMBO Rep.* **20**, e47382. doi:10.15252/embr.201847382

De Iaco, A., Verp, S., Offner, S., Grun, D. and Trono, D. (2020). DUX is a non-essential synchronizer of zygotic genome activation. *Development* **147**, dev177725. doi:10.1242/dev.177725

Eckersley-Maslin, M. A. (2020). Keeping your options open: insights from Dppa2/4 into how epigenetic priming factors promote cell plasticity. *Biochem. Soc. Trans.* **48**, 2891-2902. doi:10.1042/BST20200873

Eckersley-Maslin, M., Alda-Catalinas, C., Blotenburg, M., Kreibich, E., Krueger, C. and Reik, W. (2019). Dppa2 and Dppa4 directly regulate the Dux-driven zygotic transcriptional program. *Genes Dev.* **33**, 194-208. doi:10.1101/gad.321174.118

Eckersley-Maslin, M. A., Parry, A., Blotenburg, M., Krueger, C., Ito, Y., Franklin, V. NR., Narita, M., D'Santos, C. S. and Reik, W. (2020). Epigenetic priming by Dppa2 and 4 in pluripotency facilitates multi-lineage commitment. *Nat. Struct. Mol. Biol.* **27**, 696-705. doi:10.1038/s41594-020-0443-3

Fu, X., Zhang, C. and Zhang, Y. (2020). Epigenetic regulation of mouse preimplantation embryo development. *Curr. Opin. Genet. Dev.* **64**, 13-20. doi:10.1016/j.gde.2020.05.015

Genet, M. and Torres-Padilla, M.-E. (2020). The molecular and cellular features of 2-cell-like cells: a reference guide. *Development* **147**, dev189688. doi:10.1242/dev.189688

Gretarsson, K. H. and Hackett, J. A. (2020). Dppa2 and Dppa4 counteract de novo methylation to establish a permissive epigenome for development. *Nat. Struct. Mol. Biol.* **27**, 706-716. doi:10.1038/s41594-020-0445-1

Grow, E. J., Weaver, B. D., Smith, C. M., Guo, J., Stein, P., Shadle, S. C., Hendrickson, P. G., Johnson, N. E., Butterfield, R. J., Menafra, R. et al. (2021). p53 convergently activates Dux/DUX4 in embryonic stem cells and in facioscapulohumeral muscular dystrophy cell models. *Nat. Genet.* **53**, 1207-1220. doi:10.1038/s41588-021-00893-0

Gu, B., Posfai, E. and Rossant, J. (2018). Efficient generation of targeted large insertions by microinjection into two-cell-stage mouse embryos. *Nat. Biotechnol.* **36**, 632-637. doi:10.1038/nbt.4166

Guo, M., Zhang, Y., Zhou, J., Bi, Y., Xu, J., Xu, C., Kou, X., Zhao, Y., Li, Y., Tu, Z. et al. (2019). Precise temporal regulation of Dux is important for embryo development. *Cell Res.* **29**, 956-959. doi:10.1038/s41422-019-0238-4

Hamatani, T., Carter, M. G., Sharov, A. A. and Ko, M. S. H. (2004). Dynamics of global gene expression changes during mouse preimplantation development. *Dev. Cell* **6**, 117-131. doi:10.1016/S1534-5807(03)00373-3

Hendrickson, P. G., Doráis, J. A., Grow, E. J., Whiddon, J. L., Lim, J.-W., Wike, C. L., Weaver, B. D., Pflueger, C., Emery, B. R., Wilcox, A. L. et al. (2017). Conserved roles of mouse DUX and human DUX4 in activating cleavage-stage genes and MERVL/HERVL retrotransposons. *Nat. Genet.* **49**, 925-934. doi:10.1038/ng.3844

Hernandez, C., Wang, Z., Ramazanov, B., Tang, Y., Mehta, S., Dambrot, C., Lee, Y.-W., Tessema, K., Kumar, I., Astudillo, M. et al. (2018). Dppa2/4 facilitate epigenetic remodeling during reprogramming to pluripotency. *Cell Stem Cell* **23**, 396-411.e398. doi:10.1016/j.stem.2018.08.001

Hu, J., Wang, F., Zhu, X., Yuan, Y., Ding, M. and Gao, S. (2010). Mouse ZAR1-like (XM_359149) colocalizes with mRNA processing components and its dominant-negative mutant caused two-cell-stage embryonic arrest. *Dev. Dyn.* **239**, 407-424. doi:10.1002/dvdy.22170

Inoue, A., Chen, Z., Yin, Q. and Zhang, Y. (2018). Maternal Eed knockout causes loss of H3K27me3 imprinting and random X inactivation in the extraembryonic cells. *Genes Dev.* **32**, 1525-1536. doi:10.1101/gad.318675.118

Jin, Y., Tam, O. H., Paniagua, E. and Hammell, M. (2015). TEtranscripts: a package for including transposable elements in differential expression analysis of RNA-seq datasets. *Bioinformatics* **31**, 3593-3599. doi:10.1093/bioinformatics/btv422

Kent, W. J., Sugnet, C. W., Furey, T. S., Roskin, K. M., Pringle, T. H., Zahler, A. M. and Haussler, D. (2002). The human genome browser at UCSC. *Genome Res.* **12**, 996-1006. doi:10.1101/gr.229102

Kim, D., Langmead, B. and Salzberg, S. L. (2015). HISAT: a fast spliced aligner with low memory requirements. *Nat. Methods* **12**, 357-360. doi:10.1038/nmeth.3317

Kobayashi, W. and Tachibana, K. (2021). Awakening of the zygotic genome by pioneer transcription factors. *Curr. Opin. Struct. Biol.* **71**, 94-100. doi:10.1016/j.sbi.2021.05.013
Lan, Z.-J., Xu, X. and Cooney, A. J. (2004). Differential oocyte-specific expression of Cre recombinase activity in GDF-9-iCre, Zp3cre, and Msx2Cre transgenic mice. *Biol. Reprod.* **71**, 1469-1474. doi:10.1095/biolreprod.104.031757
Liu, B., Xu, Q., Wang, Q., Feng, S., Lai, F., Wang, P., Zheng, F., Xiang, Y., Wu, J., Nie, J. et al. (2020). The landscape of RNA Pol II binding reveals a stepwise transition during ZGA. *Nature* **587**, 139-144. doi:10.1038/s41586-020-2847-y
Love, M. I., Huber, W. and Anders, S. (2014). Moderated estimation of fold change and dispersion for RNA-seq data with DESeq2. *Genome Biol.* **15**, 550. doi:10.1186/s13059-014-0550-8
Macfarlan, T. S., Gifford, W. D., Driscoll, S., Lettieri, K., Rowe, H. M., Bonanomi, D., Firth, A., Singer, O., Trono, D. and Pfaff, S. L. (2012). Embryonic stem cell potency fluctuates with endogenous retrovirus activity. *Nature* **487**, 57-63. doi:10.1038/nature11244
Madan, B., Madan, V., Weber, O., Tropel, P., Blum, C., Kieffer, E., Viville, S. and Fehling, H. J. (2009). The pluripotency-associated gene Dppa4 is dispensable for embryonic stem cell identity and germ cell development but essential for embryogenesis. *Mol. Cell. Biol.* **29**, 3186-3203. doi:10.1128/MCB.01970-08
Maldonado-Saldivia, J., van den Bergen, J., Krouskos, M., Gilchrist, M., Lee, C., Li, R., Sinclair, A. H., Surani, M. A. and Western, P. S. (2007). Dppa2 and Dppa4 are closely linked SAP motif genes restricted to pluripotent cells and the germ line. *Stem Cells* **25**, 19-28. doi:10.1634/stemcells.2006-0269
Nakamura, T., Nakagawa, M., Ichisaka, T., Shiota, A. and Yamanaka, S. (2011). Essential roles of ECAT15-2/Dppa2 in functional lung development. *Mol. Cell. Biol.* **31**, 4366-4378. doi:10.1128/MCB.05701-11
Pertea, M., Kim, D., Pertea, G. M., Leek, J. T. and Salzberg, S. L. (2016). Transcript-level expression analysis of RNA-seq experiments with HISAT, StringTie and Ballgown. *Nat. Protoc.* **11**, 1650-1667. doi:10.1038/nprot.2016.095
Schultz, R. M., Stein, P. and Svoboda, P. (2018). The oocyte-to-embryo transition in mouse: past, present, and future. *Biol. Reprod.* **99**, 160-174. doi:10.1093/biolre/ioy013
Sun, Z., Yu, H., Zhao, J., Tan, T., Pan, H., Zhu, Y., Chen, L., Zhang, C., Zhang, L., Lei, A. et al. (2021). LIN28 coordinately promotes nucleolar/ribosomal functions and represses the 2C-like transcriptional program in pluripotent stem cells. *Protein Cell*. doi:10.1007/s13238-021-00864-5
Wang, Q. T., Piotrowska, K., Ciemerych, M. A., Milenkovic, L., Scott, M. P., Davis, R. W. and Zernicka-Goetz, M. (2004). A genome-wide study of gene activity reveals developmental signaling pathways in the preimplantation mouse embryo. *Dev. Cell* **6**, 133-144. doi:10.1016/S1534-5807(03)00404-0
Wang, H., Yang, H., Shivalila, C. S., Dawlaty, M. M., Cheng, A. W., Zhang, F. and Jaenisch, R. (2013). One-step generation of mice carrying mutations in multiple genes by CRISPR/Cas-mediated genome engineering. *Cell* **153**, 910-918. doi:10.1016/j.cell.2013.04.025
Whiddon, J. L., Langford, A. T., Wong, C.-J., Zhong, J. W. and Tapscott, S. J. (2017). Conservation and innovation in the DUX4-family gene network. *Nat. Genet.* **49**, 935-940. doi:10.1038/ng.3846
Wu, J., Huang, B., Chen, H., Yin, Q., Liu, Y., Xiang, Y., Zhang, B., Liu, B., Wang, Q., Xia, W. et al. (2016). The landscape of accessible chromatin in mammalian preimplantation embryos. *Nature* **534**, 652-657. doi:10.1038/nature18606
Yan, Y.-L., Zhang, C., Hao, J., Wang, X.-L., Ming, J., Mi, L., Na, J., Hu, X. and Wang, Y. (2019). DPPA2/4 and SUMO E3 ligase PIAS4 opposingly regulate zygotic transcriptional program. *PLoS Biol.* **17**, e3000324. doi:10.1371/journal.pbio.3000324
Yao, X., Zhang, M., Wang, X., Ying, W., Hu, X., Dai, P., Meng, F., Shi, L., Sun, Y., Yao, N. et al. (2018). Tild-CRISPR allows for efficient and precise gene knock in in mouse and human cells. *Dev. Cell* **45**, 526-536.e525. doi:10.1016/j.devcel.2018.04.021
Zeng, F., Baldwin, D. A. and Schultz, R. M. (2004). Transcript profiling during preimplantation mouse development. *Dev. Biol.* **272**, 483-496. doi:10.1016/j.ydbio.2004.05.018
Zhang, Y., Xiang, Y., Yin, Q., Du, Z., Peng, X., Wang, Q., Fidalgo, M., Xia, W., Li, Y., Zhao, Z.-A. et al. (2018). Dynamic epigenomic landscapes during early lineage specification in mouse embryos. *Nat. Genet.* **50**, 96-105. doi:10.1038/s41588-017-0003-x
Zhang, C., Chen, Z., Yin, Q., Fu, X., Li, Y., Stopka, T., Skoultchi, A. I. and Zhang, Y. (2020). The chromatin remodeler Snf2h is essential for oocyte meiotic cell cycle progression. *Genes Dev.* **34**, 166-178. doi:10.1101/gad.331157.119

Chen et al., Fig. S1

A

Loxp sites knock-in at the *Dppa2* locus

Cas9/ sgRNA1/sgRNA2/ donor DNA (ng/μl)	Injected 2-cell embryos	Transferred 2-cell (Recipients)	Pups (%)	Mice with loxp sites knock-in (%)
100/80/80/25	60	60 (3)	24 (40.0)	11/23 (47.8%)

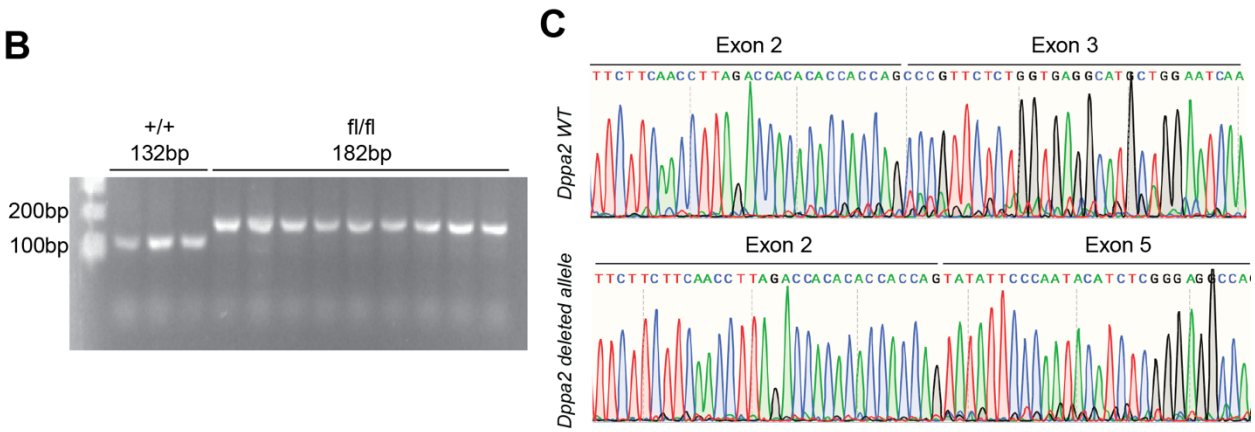

Fig. S1. Generation of *Dppa2* flox allele and CKO model

A) Summary of the microinjection and embryo transfer experiments.

B) Representative gel image for *Dppa2* flox allele genotyping.

C) Sanger sequencing data showing the Cre-mediated deletion of exon 3-4 of *Dppa2* in oocytes.

Chen et al., Fig. S2

A

Dppa2/4 in vivo E3.5 blastocysts collected after natural mating

Mating pairs	Blastocysts/litters	Blastocysts ± SD	m-z- (%)
Dppa2fl/fl × Dppa2+/-	18/3	6.0 ± 1.7	0 (0)
Gdf9-Cre,Dppa2fl/fl × Dppa2+/-	21/3	7.0 ± 1.0	9 (42.8)
Dppa4fl/fl × Dppa4+/-	19/4	4.8 ± 0.9	0 (0)
Gdf9-Cre,Dppa4fl/fl × Dppa4+/-	17/3	5.6 ± 1.5	9 (52.9)

B

Dppa4 mating summary

Mating pairs	weaning pups /litters	litter size ± SD	m+z+ (%)	m-z+ (%)	m-z- (%)
Dppa4fl/fl × WT B6	55/9	6.9 ± 2.2	55 (100)	0 (0)	0 (0)
Gdf9-Cre,Dppa4fl/fl × WT B6	66/10	6.6 ± 2.2	0 (0)	66 (100)	0 (0)
Gdf9-Cre,Dppa4fl/fl × Dppa4+/-	64/14	4.5 ± 2.5	0 (0)	61 (95.3)	3 (4.7)

Mating pairs	E18.5 pups /litters	E18.5 pups ± SD	m+z+ (%)	m-z+ (%)	m-z- (%)
Gdf9-Cre,Dppa4fl/fl × Dppa4+/-	60/9	6.6 ± 1.2	0 (0)	34 (56.6)	26 (43.4)

Dppa2 mating summary

Mating pairs	weaning pups /litters	litter size ± SD	m+z+ (%)	m-z+ (%)	m-z- (%)
Dppa2fl/fl × WT B6	28/4	7.0 ± 1.8	28 (100)	0 (0)	0 (0)
Gdf9-Cre,Dppa2fl/fl × Dppa2+/-	15/3	5.0 ± 1.0	0 (0)	15 (100)	0 (0)

Mating pairs	E18.5 pups /litters	E18.5 pups ± SD	m+z+ (%)	m-z+ (%)	m-z- (%)
Gdf9-Cre,Dppa2fl/fl × Dppa2+/-	13/2	6.5 ± 3.5	0 (0)	5 (38.5)	8 (61.5)

C

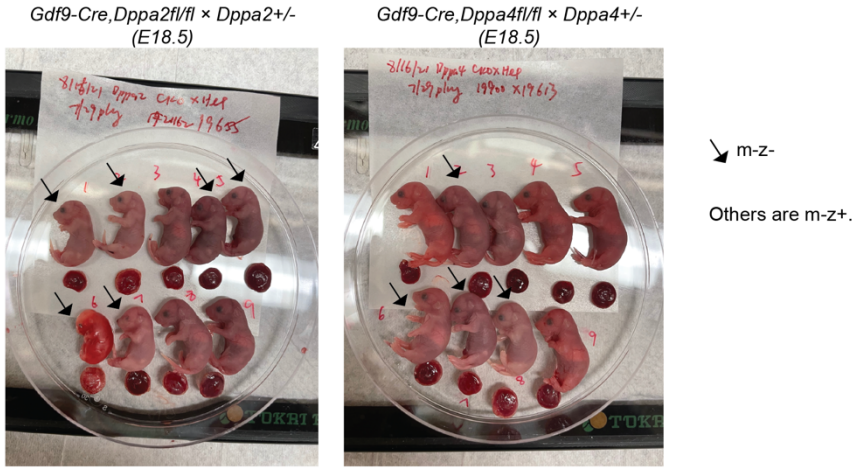

Fig. S2. Embryos without DPPA2 or DPPA4 show perinatal lethality

A) Summary of E3.5 *in vivo* blastocysts collected.

B) Mating summary of *Dppa2* and *Dppa4* mutants.

C) Representative images of E18.5 pups of *Dppa2* and *Dppa4* mutants.

Chen et al., Fig. S3

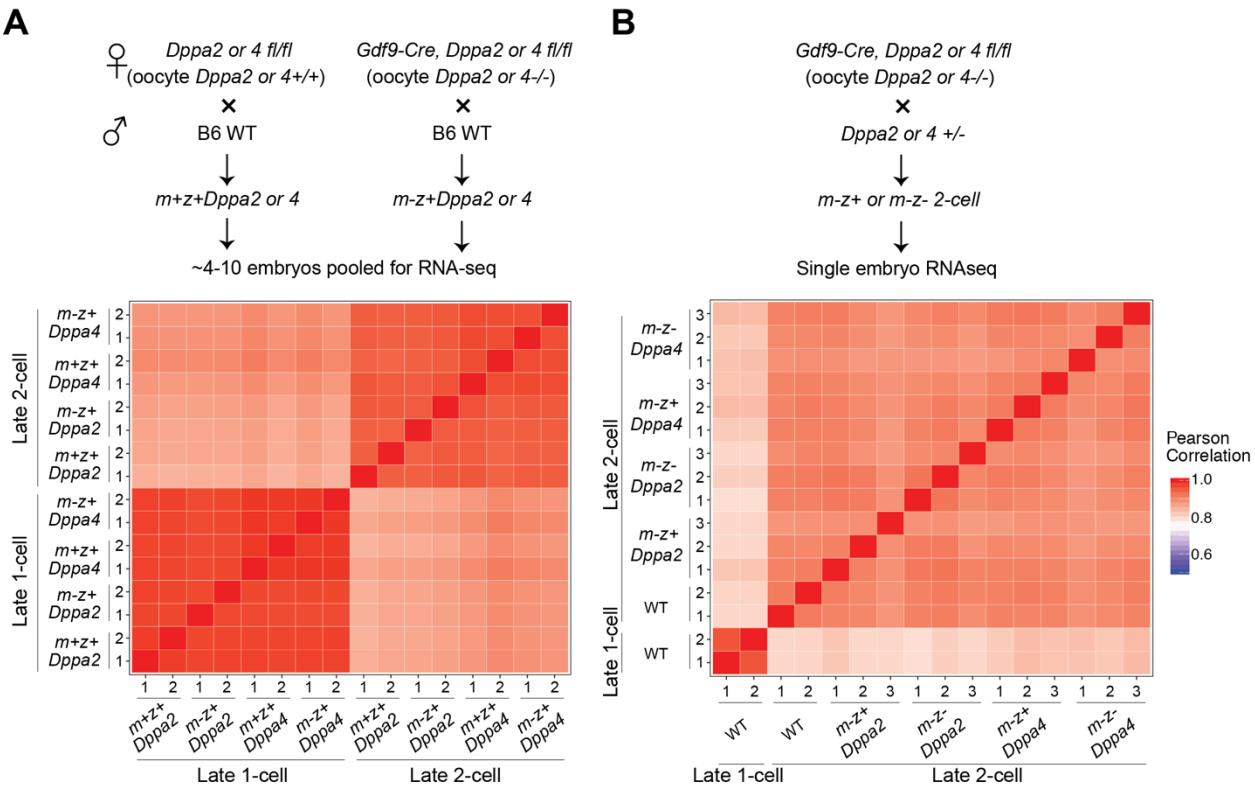

Fig. S3. Reproducibility of RNA-seq experiments

For both panels **A-B)**, top panels showing the scheme for collecting pooled or single embryos for RNA-seq and bottom panels showing the Pearson correlation heatmaps.

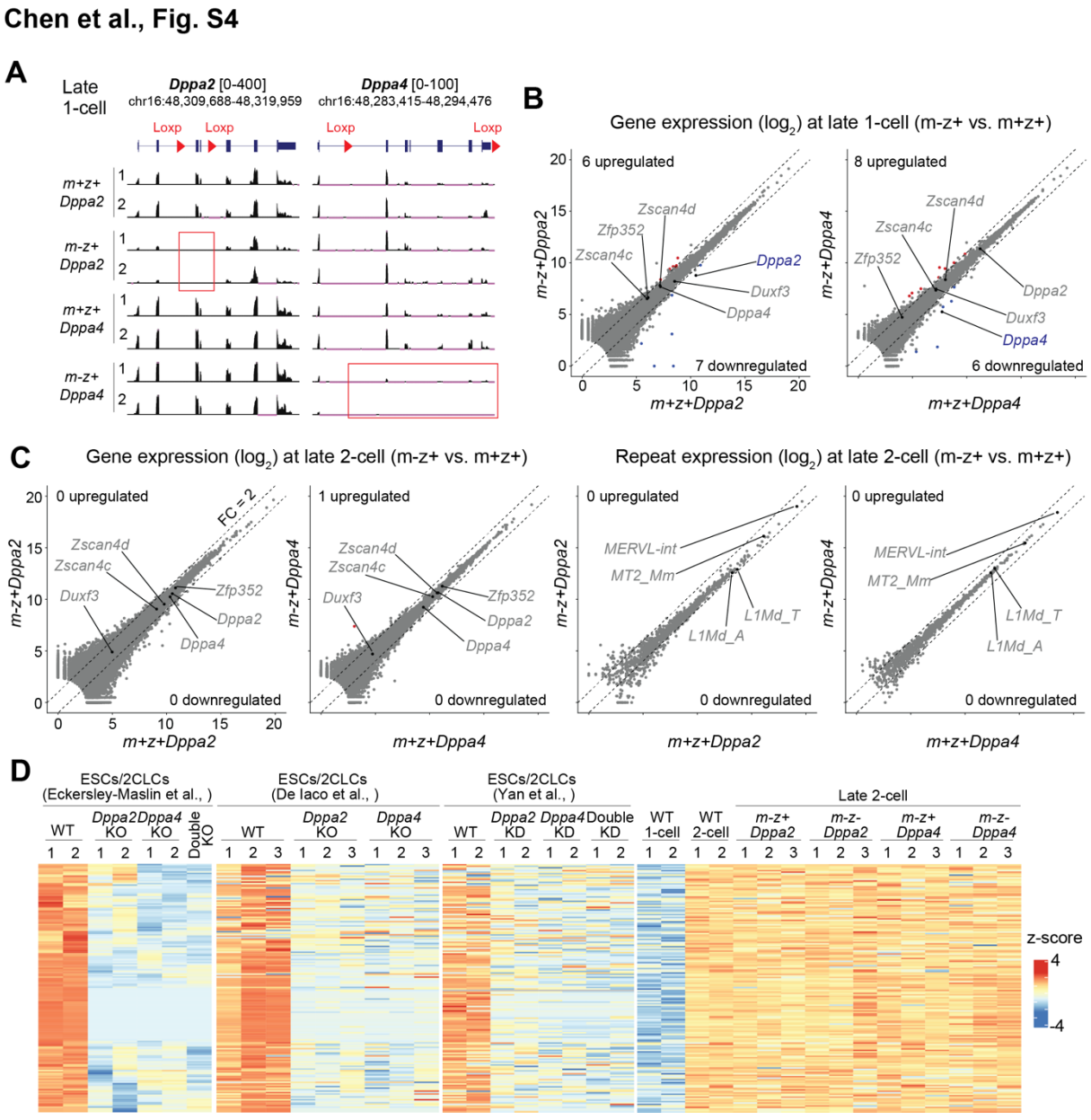

Fig. S4. Maternal DPPA2 and DPPA4 are not responsible for activating *Dux* and ZGA

A) Genome browser views of indicated RNA-seq samples at *Dppa2* and *Dppa4* loci. Cre-mediated deletion of exons are highlighted by red boxes.

B) Scatter plots comparing gene expression levels of 1-cell embryos (*m-z+* vs. *m+z+*). The x and y axes are normalized read counts by DESeq2 (log2)(Love et al. 2014). Differential gene expression criteria were fold change (FC) > 2, adjusted P-value < 0.05 and FPKM > 1. Note that the dots outside the dashed FC lines were not classified as differentially expressed because of their large P-values and/or low FPKM (**Table S1**).

C)Scatter plots comparing gene/repeat expression levels of 2-cell embryos (*m*-*z*+ vs. *m*+*z*+**).**

D) Heatmap showing the expression levels of DPPA2/4-dependent ZGA genes in ESCs/2CLCs and 2-cell embryos. ZGA genes that were down-regulated in either Dppa2 or Dppa4 KO ESCs (Eckersley-Maslin et al.,)(fold change > 2 & adjusted p-value < 0.05) were selected (n = 170).

Table S1. Differential gene expression analyses in *Dppa2* and *Dppa4* mutant embryos

Click here to download Table S1

Table S2. Summary of generated RNA-seq datasets

Click here to download Table S2

Table S3. List of primers and antibodies

Click here to download Table S3